System Identification of AMB Systems: Steps Towards Automated Commissioning

Alican Sahinkaya and Jerzy T. Sawicki
Center for Rotating Machinery Dynamics and Control (RoMaDyC)
Washkewicz College of Engineering, Cleveland State University
Cleveland, OH 44115 USA
a.sahinkaya@csuohio.edu, j.sawicki@csuohio.edu

***Abstract*— Active magnetic bearings (AMBs) are mechatronic devices that provide contact-free support to rotors via electromagnetic forces. An accurate model of the system is necessary to design and evaluate controllers for reliable operation. In this paper, identification of AMB systems is studied with the aim of reducing user involvement in the model identification process. The assumed *a priori* information consists of the amplifier model, dynamics of AMB electronics, and time delays due to AD/DA conversions, which are relatively easy to identify compared to the rotor model and AMB force model. It is also assumed that there exists a predesigned controller that stabilizes the system, not necessarily a performant one, in order to conduct system identification experiments. To obtain frequency response data for identification purposes, three common excitation signals for rotor systems are considered: impulse signal, PRBS (Pseudo-Random Binary Sequence) signal, and stepped sine signal. Feasibility of using each signal along with advantages and disadvantages over each other in obtaining accurate data in the context of commissioning is discussed. The identification problem is cast as a nonlinear least square (NLS) optimization problem using a parametrized model of an AMB system. The resulting model is physically interpretable, which allows defining uncertainties for AMB force constants and flexible mode frequencies that are standard for the model-based controller design strategies. The presented identification procedure is applied to an experimental AMB rotor system to validate the approach. A signal-based H_∞ controller is designed based on the identified model to show the applicability of the presented method for commissioning of AMB systems. Performance of the system with H_∞ controller is compared to an experimentally-tuned PID controller to demonstrate the superiority of a model-based controller, hence the importance of having an accurate plant model.**

I. INTRODUCTION

Active Magnetic Bearing (AMB) systems consist of a rotor, sensors to detect the position of the rotor, controller, power amplifiers, and magnetic actuators, where each component works together to support the rotor via electromagnetic forces. There are many different procedures presented in the literature to design a controller for an AMB system to achieve the desired performance, with the methods ranging from tuning simple PID-type controllers to designing more complicated model-based robust controllers. Since an AMB system is inherently unstable and its dynamics changes with rotational speed due to gyroscopic effects, an accurate model needs to be utilized in the design of a controller. That is why system identification of an AMB system is an important aspect of the fast and reliable commissioning process.

There are effective tools to create a model of an AMB system utilizing techniques such as finite element method (FEM). However not all physical parameters of the system can be theoretically derived, especially in the case of rotors with complex geometries and shrink fits. That is why it is necessary to either obtain or update AMB system models using experimental data, usually utilizing frequency response functions (FRFs). Lösch [1] presented an iterative procedure to identify AMB system models, where first, the rigid body model was identified to design a preliminary stabilizing controller, then the flexible modes of the model were identified using standard system identification techniques, and finally, the gyroscopic matrix was identified to create the complete AMB system model. Balini et al. [2] applied predictor-based subspace identification (PBSID) method to obtain a linear model of an AMB system, where they used the identified rigid body model to design a robust controller. Noshadi et al. [3] used genetic algorithm-based weighted least squares method to identify a desired ordered model utilizing preobtained frequency response data. Gähler et al. [4] proposed a two-step algorithm for multivariable identification of AMB systems using experimentally obtained FRFs to generate a model with pre-defined order and structure using linear least square algorithms. Wroblewski et al. [5] presented an experimentally-driven approach to model updating where the initial analytical model of an AMB supported machining spindle did not match the experimental data due to complex rotor assembly with shrink fits and squirrel cage induction motor. The approach used the knowledge of rotor assembly to select parameters of the rotor model to be tuned via optimization to account for complex dynamics that is not easy to be modeled.

However, presented methods in the literature for identification of AMB systems either require an experienced engineer to formulate the problem and perform the experiments or do not identify the complete AMB system model. That is why the aim of this study is to explore methods for identification of AMB systems, specifically the rotor-bearing model, without relying on a skilled engineer to take a step towards automated commisioning, where automated controller synthesis procedure described in [6] can be used to synthesize a controller to satisfy desired robust performance objectives.

II. AMB System Identification Problem

AMB systems consist of a rotor, magnetic actuators with built-in sensors, power amplifiers, and hardware for digital control. Figure 1 presents a simplified block diagram of a standard AMB system, where the open loop system is shown in solid lines.

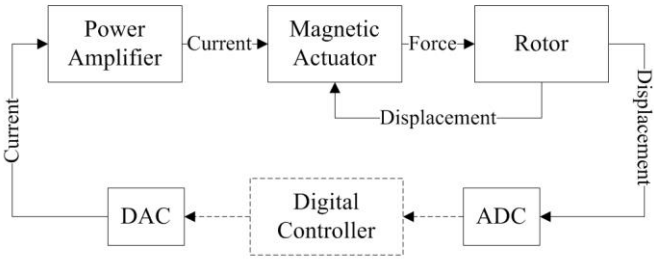

Figure 1. Block diagram of a standard AMB system

Typically, the open loop AMB system model is obtained by first deriving the rotor model using FEM. Second, magnetic actuator model is derived based on manufacturer supplied specifications and linearizing magnetic force equation around desired operating point. Lastly, the power amplifier and time delays due to ADC/DAC are modeled based on hardware specifications such as the bandwidth of the amplifiers and time delays in digital converters. The power amplifier model can also be experimentally identified with AMBs as the load to account for the effects of AMB electronics rather than modeling the AMB electronics separately. Challenges arise when a rotor with a complex assembly is to be modeled using FEM due to difficulty in representing certain features of the rotor. Also, the linear approximation of the magnetic actuator force model usually do not fully account for certain losses such as iron losses and eddy current losses. Therefore, in an attempt to minimize the above-mentioned difficulties, this study focuses on experimental identification of the rotor-bearing model, i.e., the rotor and AMB force model.

A. AMB System FRF Data Collection

The first step in AMB system identification is to obtain an open loop FRF data. Due to unstable nature of AMB systems, data for the open loop system needs to be extracted from closed loop measurements. A method from literature is utilized to obtain the MIMO frequency response data of the open loop AMB system [7, 8]. Figure 2 illustrates the experiment design where $\mathbf{P}(s)$ is the open loop system, $\mathbf{K}(s)$ is a stabilizing controller, **e** is excitation signal, **u** is supplied input to the system, and **y** is position sensor output from the built-in AMB sensors.

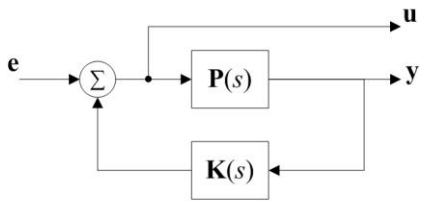

Figure 2. Experiment design for obtaining open loop FRF data for AMB system identification

From Fig.2, the relation between the excitation signal **e** and output signals **u** and **y** can be obtained as

$$\mathbf{u}(s) = [\mathbf{I} - \mathbf{K}(s)\mathbf{P}(s)]^{-1}\mathbf{e}(s) = \mathbf{S}(s)\mathbf{e}(s)$$
$$\mathbf{y}(s) = \mathbf{P}(s)[\mathbf{I} - \mathbf{K}(s)\mathbf{P}(s)]^{-1}\mathbf{e}(s) = \mathbf{G}(s)\mathbf{e}(s)$$

Then, the desired open loop system model can be constructed as

$$\mathbf{P}(s) = \mathbf{G}(s)\mathbf{S}^{-1}(s)$$

Note that the excitation input signal needs to be chosen carefully to make sure the existence of required inverses. Moreover, each column of $\mathbf{S}(s)$ and $\mathbf{G}(s)$ needs to be measured independently, i.e., for an AMB system with 4 inputs, at least 4 separate experiments are required to obtain $\mathbf{P}(s)$. The required frequency response data are obtained using the built-in actuators and sensors of the AMBs via the use of carefully designed excitation signal.

B. Excitation Signal Design

Three commonly used force excitation signals for identification of rotating machinery are considered in this study: impulse signal, PRBS (Pseudo-Random Binary Sequence) signal, and stepped-sine signal. Although each signal can produce satisfactory results in theory, each type brings certain limitations to the experiment and hence their limitations should be identified to select the best excitation signal to automate AMB system identification process.

Impulse signal has the advantage of exciting all frequencies at once. However, the signal might not be able to cause the rotor to move significantly due to limit on maximum current that can be supplied to the system and the duration of the signal which defines the frequency content. That's why impulse signal usually results in poor signal-to-noise ratio, hence result in noisy FRF. Stepped-sine signal, on the other hand, offers the option to change the magnitude of the excitation signal depending on the frequency to adjust signal-to-noise ratio as desired. However, the experiment might take too long to collect data for the desired high density frequency grid. PRBS signal has the advantage of being able to consistently excite the system to obtain data for a high-density frequency grid with enough power that usually results in high signal-to-noise ratio. However, the frequency response data might still get corrupted due to noise. Considering the advantages and disadvantages of each signal, PRBS signal is determined to be the best option mainly due to ease of design, resulting high-density frequency data, and the required time for the experiments.

C. Identification Problem Formulation

Once the frequency response data is obtained, a model can be fit to the data using one of many methods described in literature such as prediction error method (PEM) [9], subspace state-space system identification (N4SID) [10], and rational fraction polynomial (RFP) method [11]. However, these methods require an experienced engineer to formulate the problem to achieve acceptable results. That is why in order to reduce the identification procedures dependency on the user, a grey-box like approach is proposed where the

model fitting is cast as a nonlinear least square (NLS) problem and solved by NL2SOL algorithm [12].

Expected modal model structure of a nonrotating AMB system with two radial bearings for a single plane, excluding amplifier, power electronics, and time delay models, has the following state-space matrices:

$$\mathbf{A}_x = \begin{bmatrix} \mathbf{0} & \mathbf{I} \\ \mathbf{w} & \mathbf{d} \end{bmatrix} + \begin{bmatrix} \mathbf{0} & \mathbf{0} \\ \mathbf{b}_{\mathrm{DE}} & \mathbf{b}_{\mathrm{NDE}} \end{bmatrix} \begin{bmatrix} k_{\mathrm{x1}} & 0 \\ 0 & k_{\mathrm{x2}} \end{bmatrix} \begin{bmatrix} \mathbf{c}_{\mathrm{DEa}} & \mathbf{0} \\ \mathbf{c}_{\mathrm{NDEa}} & \mathbf{0} \end{bmatrix}$$

$$\mathbf{B}_x = \begin{bmatrix} \mathbf{0} & \mathbf{0} \\ \mathbf{b}_{\mathrm{DE}} & \mathbf{b}_{\mathrm{NDE}} \end{bmatrix} \begin{bmatrix} k_{\mathrm{i1}} & 0 \\ 0 & k_{\mathrm{i2}} \end{bmatrix}, \quad \mathbf{C}_x = \begin{bmatrix} \mathbf{c}_{\mathrm{DEs}} & \mathbf{0} \\ \mathbf{c}_{\mathrm{NDEs}} & \mathbf{0} \end{bmatrix}, \quad \mathbf{D}_x = \mathbf{0}$$

where **w** is a diagonal matrix containing rigid and flexible mode frequencies, **d** is a diagonal matrix containing modal damping information, k_{i1} and k_{i2} are current stiffness values of drive end (DE) and non-drive end (NDE) bearing actuators respectively, k_{x1} and k_{x2} are position stiffness values of DE and NDE bearing actuators respectively, $\mathbf{b}_{\mathrm{DE}}$ and $\mathbf{b}_{\mathrm{NDE}}$ represents input matrices for DE and NDE bearings respectively, $\mathbf{c}_{\mathrm{DEs}}$ and $\mathbf{c}_{\mathrm{NDEs}}$ are output matrices for DE and NDE position sensors respectively, and $\mathbf{c}_{\mathrm{DEa}}$ and $\mathbf{c}_{\mathrm{NDEa}}$ are output matrices for positions at actuator locations for DE and NDE bearings respectively, which are typically not equal to $\mathbf{c}_{\mathrm{DEs}}$ and $\mathbf{c}_{\mathrm{NDEs}}$ due to non-collocation of sensors and actuators of AMBs. If the AMBs of the system are identical and the rotor is symmetric, some simplification can be made such as bearing stiffness constants, k_{x} and k_{i}, can be set to the same values for the DE and NDE bearings and two planes of the AMB system can be considered identical.

The cost function for the NLS problem is chosen to be the weighted sum of squared values of the difference between the experimentally obtained FRF data and fitted model frequency response. The only user involvement in this framework is to define the number of flexible modes in the relevant frequency region, identify parts of the data that correspond to resonances and anti-resonances, and identify parts of the data that are corrupted by noise. The weights for parts around resonances and anti-resonance are set to be 30, parts corrupted by noise are set to be 0.1, and the rest are set to be 1. The calculated errors are converted to dB before applying the weights to reduce the magnitude difference within the error vector. Since there is no unique solution to this problem, bearing constants cannot be identified separately.

Gyroscopic matrix **G** is identified after identifying the nonrotating AMB system model. The full AMB system can be constructed as a two decoupled systems coupled by the gyroscopic matrix **G** and is modeled as;

$$\mathbf{A} = \begin{bmatrix} \mathbf{A}_{\mathbf{x}} & \mathbf{0} \\ \mathbf{0} & \mathbf{A}_{\mathbf{y}} \end{bmatrix} + \Omega \begin{bmatrix} \mathbf{0} & -\mathbf{G} \\ \mathbf{G} & \mathbf{0} \end{bmatrix},$$

$$\mathbf{B} = \begin{bmatrix} \mathbf{B}_x & \mathbf{0} \\ \mathbf{0} & \mathbf{B}_y \end{bmatrix}, \quad \mathbf{C} = \begin{bmatrix} \mathbf{C}_x & \mathbf{0} \\ \mathbf{0} & \mathbf{C}_y \end{bmatrix}, \quad \mathbf{D} = \mathbf{0}$$

where Ω is the rotational speed of the rotor. The main effect introduced by the gyroscopic effects is the bifurcation of natural frequencies of the rotor. The amount of bifurcation is determined by the rotational speed of the rotor and the ratio of its transverse moment of inertia and polar moment of inertia. This means that a controller for the AMBs should be designed to compensate for the change in the natural frequencies of the system to prevent any possible instability and hence gyroscopic matrix needs to be identified accurately. Similar to the identification of nonrotating AMB system model, NLS problem is formulated and solved using the same weights for the cost function, where only the gyroscopic matrix is the unknown since the nonrotating AMB system matrices were found in the previous step.

III. CONTROLLER DESIGN

In order to show the validity of the identification method and to show how the identified model can be used to synthesize controllers, a signal-based H_∞ controller is designed using automated H_∞ controller design method described in [6]. The procedure is briefly described in this section for completeness.

The standard control configuration is shown in Fig. 3, where **P** is the generalized plant and **K** is the controller to be designed. In the standard control configuration, the vector **w** represents exogenous inputs to the system, such as expected disturbances acting on the system, reference trajectory, and expected sensor noise, and the vector **z** represents the outputs of the system to be regulated, such as tracking errors, vibrations of the system, and control input magnitudes.

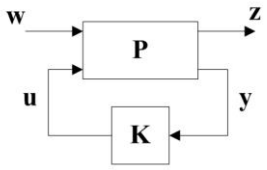

Figure 3. Standard control problem formulation

In H_∞ control problem, the vectors **w** and **z** have a 2-norm of unity and their expected values are represented by the weights embedded within the generalized plant **P**. The purpose of H_∞ control is to internally stabilize the closed loop system while minimizing the H_∞ norm of the closed loop transfer function from exogenous input **w** to performance output **z**. Depending on the selection of signals for **w** and **z**, the H_∞ control problem can be formulated either as mixed-sensitivity problem to shape selected closed-loop transfer functions or as signal-based H_∞ control problem to regulate output signals that are stacked in the vector **z** under sinusoidal excitations through the signals stacked in the vector **w.** In this study, the latter controller design approach is used since signal-based H_∞ control is more suited for control problems where multiple control objectives need to be satisfied. The formulation of signal-based H_∞ control problem can be extended to include uncertainties in the plant model by simply adding additional input-output signals that represent the given uncertainty.

For the AMB system studied, a standard disturbance rejection control problem is formulated using signal-based H_∞ control approach. Figure 4 shows the problem formulation block diagram where $\overline{\mathbf{G}}$ is the uncertain plant model, $\mathbf{W_d}$ and

$\mathbf{W_n}$ are weights that represent the expected frequency content of disturbance forces (in units of Amps since the identified model is from control current input to position output) and sensor noise respectively, and $\mathbf{W_u}$ and $\mathbf{W_p}$ are weights representing the desired control input magnitudes and vibrations at sensor locations respectively.

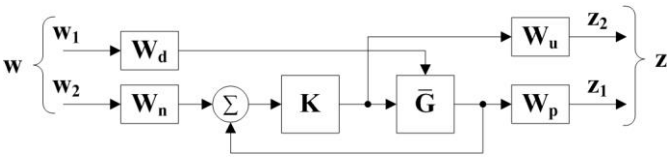

Figure 4. Signal-based H_∞ control problem formulation

The procedure to synthesize the controller described in [6] utilizes μ-analysis for robust performance in the selection of weights to achieve desired performance [13]. In the procedure, the user defines the control objectives via weights, which are referred to as analysis weights in the approach, and the uncertainties in the plant model. The procedure then casts the weight tuning process as an optimization problem, where the cost function is the μ-value of the closed-loop system with analysis weights. The cost function also includes a penalty term for unstable controllers to make sure the synthesized controller is stable. The optimization problem is then solved by genetic algorithm, where the algorithm finds weights to be used in controller synthesis that results in a μ-value of less than unity, implying that the controller achieves robust performance for the given control problem.

IV. Experimental Results

A. *Experimental AMB System*

The presented identification framework is applied to an experimental AMB system manufactured by Revolve Magnetic Bearings, subsidiary of SKF, pictured in Fig. 5. The AMB system consists of two radial AMBs which are referred to as drive end (DE) and non-drive end (NDE) bearing, one thrust AMB, a configurable rotor, and a brush type DC motor. The radial AMBs apply forces to the rotor in two perpendicular directions at 45 degrees with respect to the vertical axis. Each radial AMB is equipped with a touchdown bearing to provide a resting place for the rotor and to prevent damage to the system in the event of a failure. The touchdown bearings have a radial clearance of about 190 µm.

Figure 5. Experimental AMB system

The rotor configuration for this study is chosen to have the first four flexible modes (90 Hz, 252 Hz, 510 Hz, 730 Hz) within the manufacturer supplied bandwidth of the actuators, around ~720 Hz to make sure the presented method works for flexible rotors. The solid shaft is made of stainless steel with a diameter of 9.525 mm and length of 457.2 mm. The AMB rotors and disk are attached to the shaft via tapered sleeves. The controller unit for the AMB system has a sampling frequency of 10 kHz. Data acquisition and controller implementation are done using dSPACE hardware.

In order to obtain open loop frequency response data, a preliminary low stiffness PID controller is experimentally tuned to provide stable levitation with 1 Amp bias current, which means the identified model is valid for only 1 Amp bias and the identification procedure needs to be repeated for different bias current values. For the excitation, a 12th order PRBS signal with 5 kHz clock speed and 4 periods is designed, which allows the whole data collection procedure to take place in less than a minute and the signal provides a high-density frequency grid with ~1.22 Hz frequency steps. A sampling rate of 10 kHz is used to collect the data during the identification experiments. The first period of the PRBS signal is omitted for the post-processing to remove the transient response from the collected data. Same excitation signal is used to collect data for both nonrotating and rotating case. The experiment to collect data is performed following simple steps; first, energize the AMBs to levitate the rotor, and then after transients died out, apply excitation to DE x-axis, NDE x-axis, DE y-axis, and lastly, NDE y-axis while waiting in between for transients to die out. The position measurements for the whole experiment for nonrotating AMB system identification is shown in Fig. 6 and the sum of the control currents and excitation signal are shown in Fig.7.

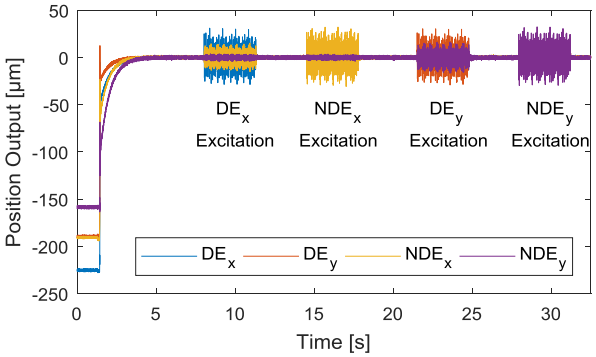

Figure 6. Position measurements during nonrotating AMB system identification experiment

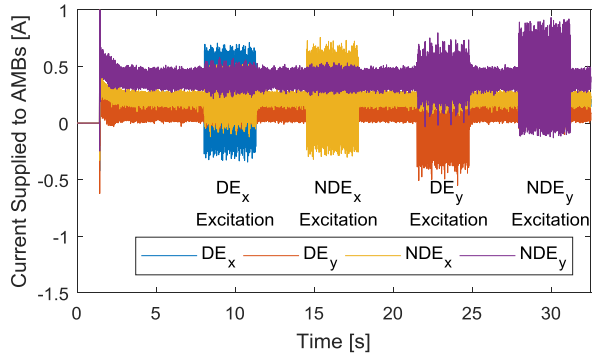

Figure 7. Current supplied to AMBs (excluding the bias current) during nonrotating AMB system identification experiment

One thing to pay attention to in Fig. 7 is the difference in control current values in x-axis and y-axis of the NDE bearing during simple levitation, i.e., the data between 5 seconds and 6 seconds in Fig. 7. The difference is more clearly shown in Table I. Since the rotor is symmetric and NDE AMB bearing is identical for both x and y-axis, it is expected for both axes to have similar, if not the same, control current magnitudes. The existence of a difference can be utilized to identify possible faults in the system and might help to interpret the observed behavior of the system. One of the possible reasons behind the observed difference is lack of alignment of the motor shaft center, DE bearing center, and NDE bearing center. The studied system is reconfigurable and the AMB housings and motor are hand tightened, which might cause them to be slightly tilted. Also, the controller uses the sensors to determine the bearing center and any bias error in sensor calibration might contribute to misalignment. However, these issues have no significant impact on the identification framework described in this study.

Once the measurements are collected for nonrotating AMB system, the method from Section II.A is utilized to extract the open loop AMB system frequency response data from closed loop measurements. Certain assumptions are made before identifying the model by observing obtained open loop frequency response data as well as knowing identical AMBs are used both for DE and NDE bearings. In the experimental setup, the DE and NDE radial AMBs are identical and the bearing constants are assumed to be the same. The experimental data showed identical behavior for two perpendicular planes of the rotor, referred to as x and y, hence the models for the two perpendicular planes are assumed to be the same as well. After these simplifications, the desired parametrized AMB system model is constructed with the knowledge that 4 flexible modes are within the bandwidth of the actuators (~720 Hz), which is apparent from the experimental data. With these assumptions, the parametrized AMB model has 46 unknown parameters. Important regions are selected to be ± 5 Hz around the peaks and valleys of each frequency response channel to apply the weight of 30 and parts of the data corrupted by noise are chosen to be between 300 Hz to 480 Hz and 540 Hz to 640 Hz for the DE input - NDE output frequency response data to apply the weight of 0.1. The NLS problem is solved using the data for only one plane due to the symmetry of the system. The comparison of the frequency response of one of the identified model, which is generated by the optimization procedure, and the experimental data for x-axis input and x and y-axis output is shown in Fig. 8. Due to the symmetry of the studied AMB system, the frequency response data for the other half of the AMB model, in other words, frequency response for y-axis inputs, was comparable to x-axis inputs, with some negligible differences that can be associated with the nature of experimental research. That is why only half of the model is presented further in the paper which seems sufficient to validate the presented identification method.

In nonrotating case, theoretically, there should be no cross-coupling term (assuming no noise). However, it is clear from Fig. 8 that there is cross-coupling between the two perpendicular axes of the system where magnitude is above the noise level which is around 1 µm/A. However the cross-coupling is significant primarily at natural frequencies. Possible reason for the presence of cross-coupling of x and y-axis might be due to the cross-coupling stiffness of the flexible coupling element between the rotor and motor. Another unexpected behavior in the frequency response data shown in Fig. 8 is the existence of local jumps in magnitude for DE_x input – DE_x output around 400 Hz and NDE_x input – NDE_x output around 650 Hz. The reason behind the cross-coupling and the local jumps in the frequency response data are considered unmodeled dynamics in this study and treated as a disturbance for controller synthesis purposes.

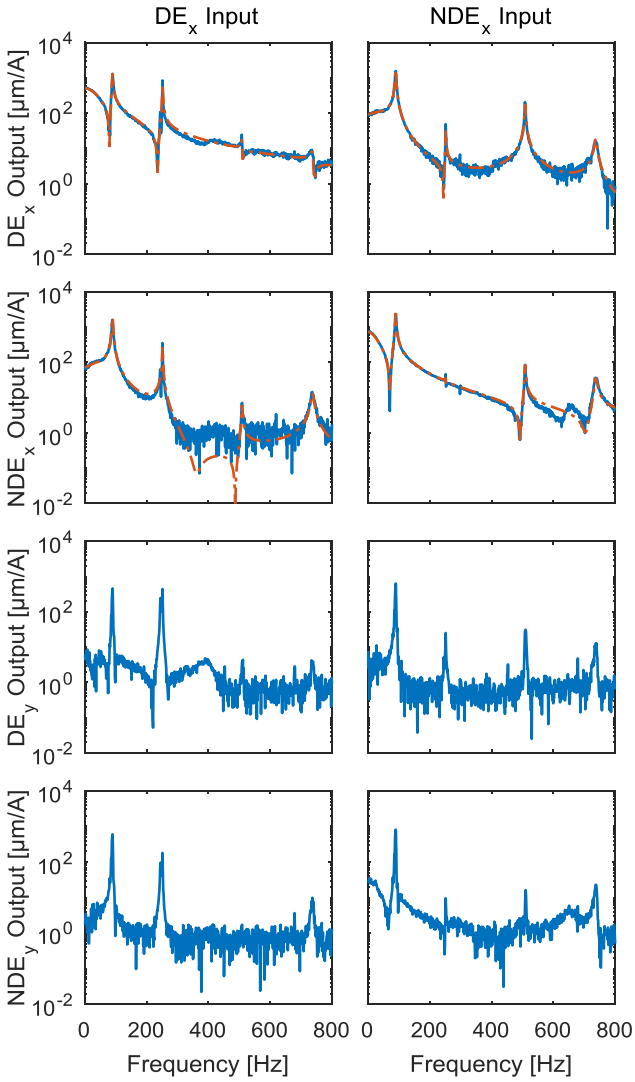

Figure 8. Comparison of identified model (dashed-red) and open loop FRF data (solid-blue)

Although Fig. 8 shows acceptable agreement between model and data for a single plane, further verification is done by comparing time response of the model to make sure the effects of unmodeled dynamics are rather negligible. For this purpose, the response of the AMB system in DE and NDE x-axis to PRBS signal applied to DE x-axis is compared to the

identified model response and is shown in Fig. 9. Time response comparison of the closed-loop identified model and physical system also shows that the identified open loop model is accurate. There are slight differences in magnitudes however these can be explained by disturbances acting on the system that are not simulated such as the AMB sensor noise and/or unmodeled dynamics.

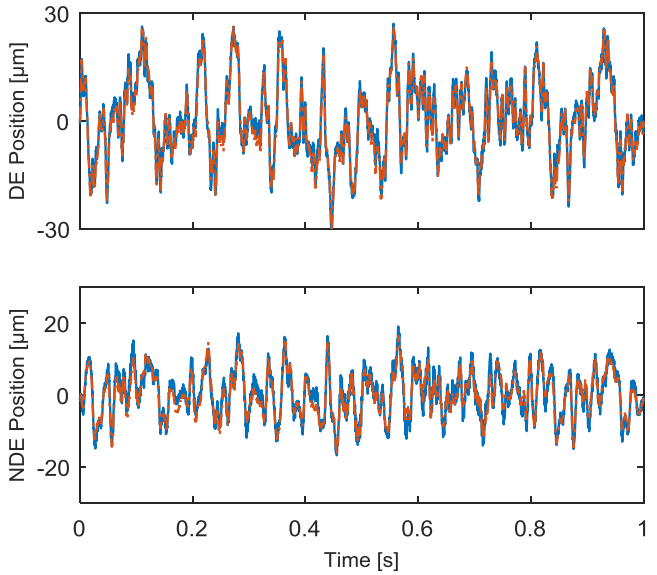

Figure 9. Comparison of closed loop x-axis response of the identified model (dashed-red) and physical system (solid-blue) to a PRBS excitation applied to x-axis of DE bearing

Since the nonrotating AMB system model is obtained with acceptable accuracy, next step to finalize the identification process is to identify the gyroscopic matrix. For this purpose, similar procedure used in identification of nonrotating AMB system is applied to the rotating AMB system at 3000 rpm. Although the run speed is chosen arbitrarily for this study, in reality it should be chosen such that gyroscopic effects are clearly seen in the system response. With 4 flexible modes included in the nonrotating AMB model, there are 25 unknown parameters that define the gyroscopic matrix, which are identified through the NLS problem described in Section II.C. Since the cross-coupling terms were not reliable due to unmodeled dynamics for the system studied, they are not used in the cost function. Also data below 50 Hz, which corresponds to rotational speed of the rotor during experiments, is omitted for the optimization process due to possible noise related issues. Figure 10 illustrates the comparison of the open loop frequency response data obtained while the rotor was running at 3000 rpm, which is extracted from the closed loop measurements using the method described in Section II.A, to the model generated via the NLS optimization. The bifurcation of flexible modes due to gyroscopic effects is clear for the 3rd and 4th flexible modes, both in experimental frequency response data and identified model output in Fig. 10, which verifies that the gyroscopic matrix is identified correctly. However there is a clear mismatch in cross-coupling terms. Although the reason behind the mismatch is not obvious, it might still be considered an acceptable match given that there was cross-coupling in nonrotating case, which implies the existence of unmodeled dynamics for the given system.

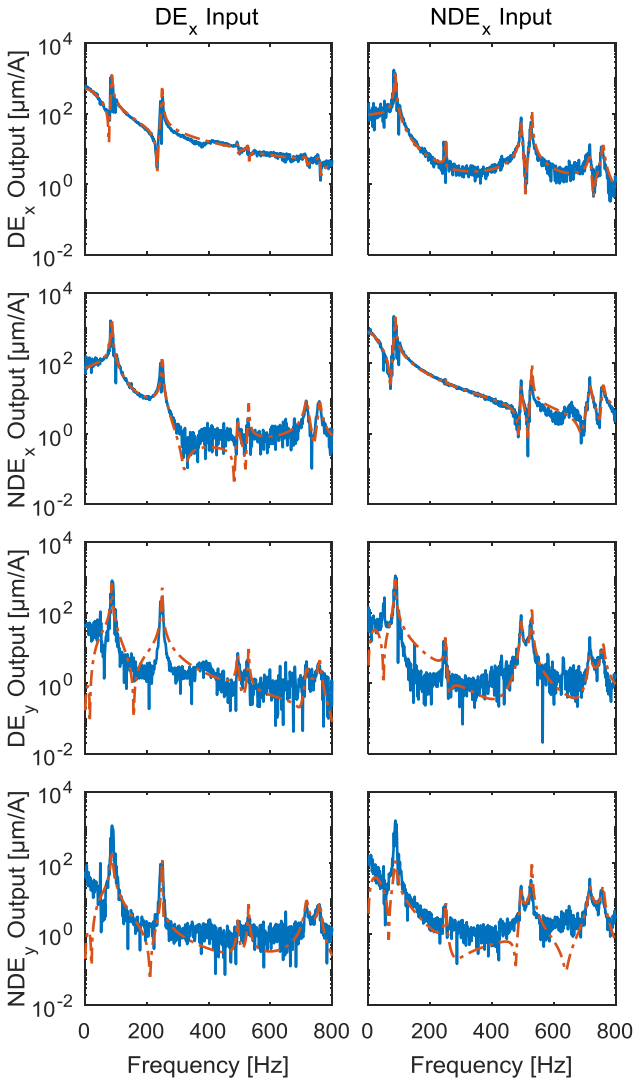

Figure 10. Comparison of identified model (dashed-red) and open loop frf data (solid-blue) obtained at 3000 rpm

Having the gyroscopic matrix identified, the full speed dependent model of the AMB system is completed. As a last verification step to determine if the model truly represents the physical system, a new measurement from the AMB system running at 1600 rpm is collected using the same PRBS signal as excitation signal and open loop FRF data is extracted from the closed-loop measurements using the method described in Section II.A. The obtained data is then compared with the speed-dependent model at 1600 rpm and the comparison is shown in Fig. 11. As expected, the bifurcations of the 3rd and 4th flexible modes are still apparent at 1600 rpm and the amount of bifurcation is less compared to 3000 rpm case. There is still mismatch on the cross-coupling terms however the flexible mode frequencies match almost perfectly, which is an indication that the gyroscopic matrix is identified correctly.

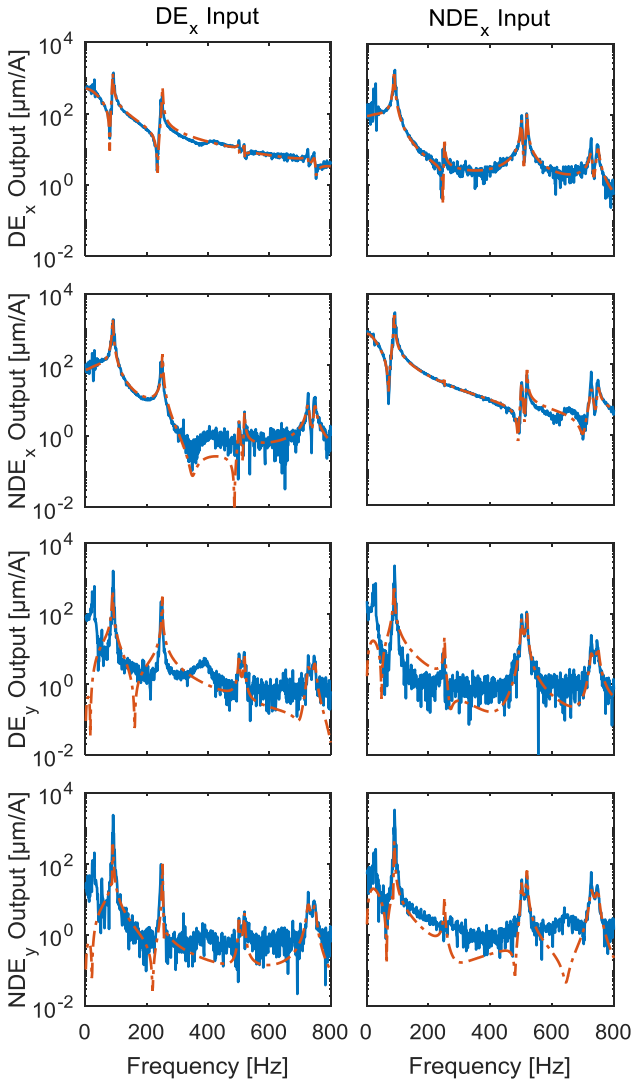

Figure 11. Comparison of identified model (dashed-red) and open loop frf data (solid-blue) obtained at 1600 rpm

There are a few limitations of the proposed identification method. First, the NLS problem is often not easy to solve, requires solving the problem multiple times with different initial guesses due to solutions dependency on the initial guess, and takes around 30 minutes to find an acceptable solution to construct the full model of the studied AMB system, and solutions are not identical mainly due to noisy measurements. However all solutions result in models that are in relatively acceptable agreement with the experimental data, for both the frequency response and time response. Second, the bearing constants are not identified separately which prevents the user from defining performance objectives using units of force or defining uncertainties for the AMB bearing force constants. However this is not a problem since they can be defined in a way that represents a physical meaning such as a percentage of maximum load capacity of the bearings and percent uncertainty of the bearing constants as multiplicative uncertainty in relevant channels.

B. Automated Controller Synthesis for the AMB System

With the results shown in Figs. 8-11, the identified speed-dependent AMB rotor system model can be considered an accurate approximation of the real physical system. However, it is not quite the same due to the existence of unmodeled dynamics and errors associated with the nature of experimental research. That is why some uncertainties need to be defined for controller synthesis to make sure that the physical model is captured within the set of plants defined by the nominal model, which is the identified full model of the AMB system, plus the defined uncertainties. One advantage of the presented identification method in this paper is the ability to easily define uncertainties. The flexible mode frequencies and flexible mode damping are already identified individually and desired uncertainties can be defined directly. However, this is not the case for the AMB force constants since they are not identified individually. However, multiplicative uncertainties can be defined as an alternative at corresponding channels to mimic the same physical meaning. For the system studied, since the PRBS signal creates a frequency grid with ~1.22 Hz steps, $\pm$2 Hz uncertainties are defined for the flexible mode frequencies. For the flexible mode damping values, since experimental data usually is not reliable to identify damping accurately, 50% uncertainty is defined to make sure the real system damping values are covered with the uncertainty. Lastly, 5% uncertainty is defined for both current and position stiffness constant of AMBs due to identified models gain matching the experimental data excluding the unmodeled dynamics. The current stiffness uncertainty is defined as uncertainty in the gain of the system and position stiffness uncertainty is defined for the c_{DE_a} variable.

The performance objective for the studied AMB system is chosen as a standard disturbance rejection objective, which means to contain the orbits with in a circle of desired radius under the influence of residual unbalance. For the studied system, the objective of control is chosen to keep vibration magnitudes less than 36 µm without saturating the AMB actuators up to maximum design speed of 6000 rpm in the presence of 1 µm sensor noise and disturbance forces which is mainly the unbalance force. Additionally, during simple levitation without rotation, the vibrations should not exceed 7 µm. Since the bearing current stiffness is not identified separately, the disturbance forces cannot be defined in units of Newtons. However, there is no issue with defining disturbance forces in units of Amps since the identified system is from control current in Amps to position in µm. One way of defining disturbance forces is to set them to some percentage of maximum capacity of the AMB bearings. For this study, the amount of disturbance forces acting on the studied system is estimated by observing control current magnitudes. For this purpose, an experimentally tuned decentralized PID controller is designed to satisfy the performance objective, where the PID controller includes a lead-lag filter to stabilize the 3rd flexible mode and a notch filter to stabilize the 4th flexible mode. The AMB system, with the PID controller, is run at various speeds and the control current magnitude spectrum at running frequency is

observed, which is obtained by simple Fourier Transform for multiple speeds including the maximum design speed of 6000 rpm. The observed values are tabulated in Table I. Although the magnitudes do not correspond exactly to the actual disturbance forces acting on the system, it can be used as a rough estimate.

Table I. OBSERVED CONTROL CURRENT MAGNITUDES UNDER VARIOUS ROTATIONAL SPEEDS WITH PID CONTROL

	DE_x [A]	DE_y [A]	NDE_x [A]	NDE_y [A]
0 rpm	0.2078	0.0682	0.1540	0.3969
1600 rpm	0.0142	0.0135	0.0798	0.0793
3000 rpm	0.1384	0.1441	0.1291	0.1382
6000 rpm	0.2786	0.2754	0.1804	0.2058

As mentioned in Section III.B, there is significant difference in control current magnitudes of the two perpendicular axes of the same bearing for nonrotating levitation, mostly due to misalignment between motor shaft center, DE bearing center, and NDE bearing center.

Analysis weights for disturbance forces are defined using the values shown in Table I, excluding the nonrotating (0 rpm) case values, and increasing them by 5% to compensate for unmodeled dynamics and to prevent underestimating the disturbance forces since PID controller does not fully cancel out the disturbance forces. Since a sharp decrease in disturbance magnitude is necessary after the frequency corresponding to the maximum design speed, Chebyshev type II filter is used instead of usual first or second order filter for roll off. The weights for the sensor noise are set to be a constant 1 µm through all frequencies and the weights for the control current magnitudes are set to be 1 Amp up to the bandwidth allowed by the hardware and rolls off afterward via the use of a second-order filter. As for the vibration levels, a first order filter is used where the magnitude is set to be 36 µm after 0.1 Hz as per objective, however, for lower frequencies it is set to be 0.7 µm instead of 7 µm to compensate for not representing the DC component for the disturbance force accurately. After defining the analysis weights, the algorithm from [6] is used to design the controller, which results in a controller with 48 states. Frequency response comparison of the experimentally tuned decentralized PID controller and the H_∞ controller is shown Fig 12, where the other half is comparable to the shown frequency response due to the symmetry of the AMB system studied.

To show the advantage of using the model-based controllers over the PID controller, hence the importance of having an accurate system model, orbits at various speeds, up to maximum design speed of 6000 rpm for the studied AMB system are shown in Fig. 13, where the PID controller is tuned experimentally to achieve the defined performance objective.

It is clear from Fig. 13 that the H_∞ controller performs better than the PID controller at all speeds. One interesting observation is at 6000 rpm. The orbit shape for the NDE bearing at 6000 rpm gets warped into a diamond shape, both for PID control and H_∞ control, where it is more apparent for the latter. This indicates a strong 3X component in the vibration signal. Possible reason for the orbits changing their shape from relatively circular to a diamond-like shape is the already mentioned misalignment between the motor shaft center, DE bearing center, and NDE bearing center.

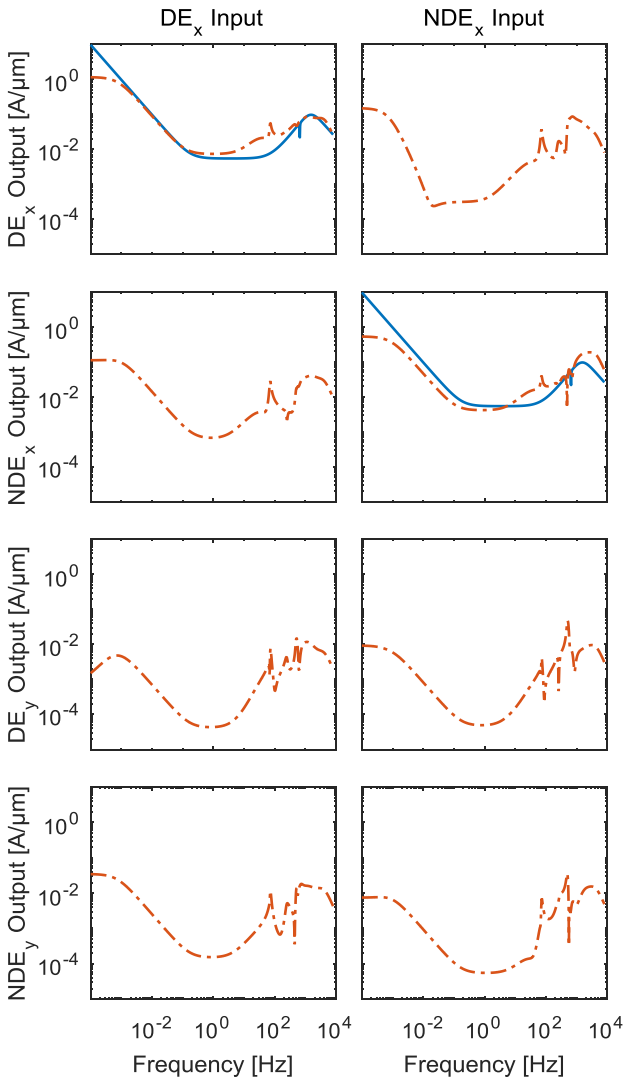

Figure 12.Frequency response of decentralized PID controller (solid-blue) and H_∞ controller (dashed-red)

I. CONCLUSION

This paper presented a method to identify an AMB system model that aims to reduce the user involvement in commissioning process. First, the AMB model is parametrized to be able to formulate the identification problem as a nonlinear least squares (NLS) problem. Second, the design of identification experiments for an AMB system is explained, where different excitation signals are considered and their feasibility is discussed to determine the best option, which is determined to be the PRBS signal. Third, the model is identified using a NLS solver and the model response is compared to the physical response of the system to check the accuracy of the identified model. Results show the validity of the presented identification procedure. Lastly, to show that the identified model can be used in robust controller

synthesis, a robust signal-based H_∞ controller is designed using the identified model and the performance of the controller is compared with an experimentally-tuned decentralized PID controller. Comparison of the achieved orbit sizes confirms the superiority of the model-based control strategy, hence the importance of accurate identification of AMB systems.

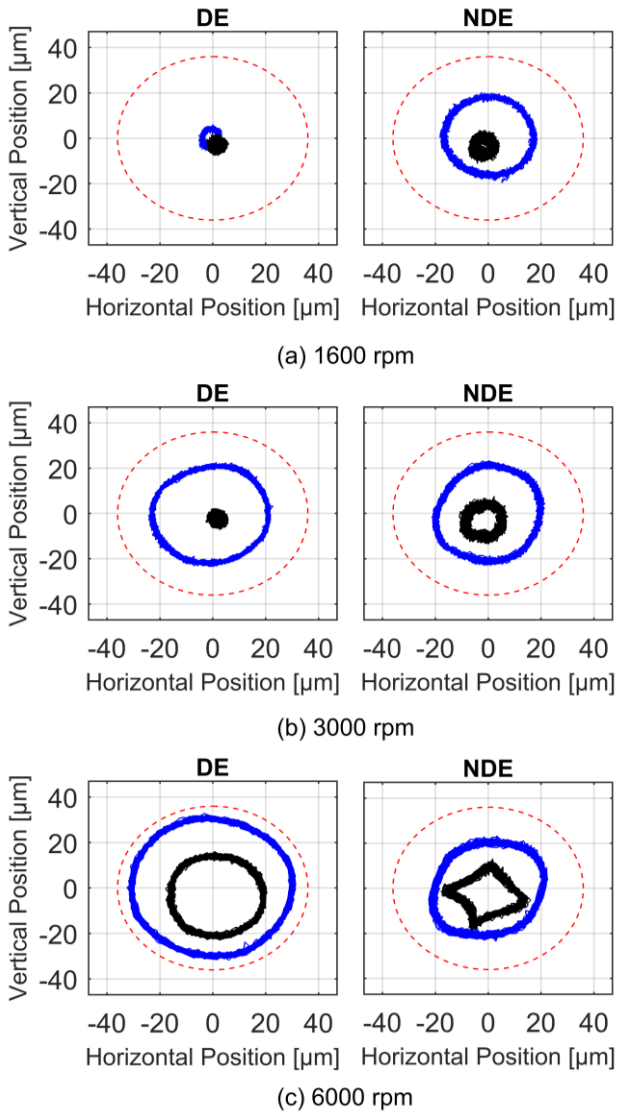

Figure 13. Orbit size comparison between PID control (blue), H_∞ control (black), and performance objective (red)

REFERENCES

[1] F. Lösch, *Identification and automated controller design for active magnetic bearing systems*, Diss. ETH. Nr. 14474, ETH Zurich, 2002.

[2] H.M.N.K. Balini, I. Houtzager, J. Witte and C.W. Scherer, "Subspace identification and robust control of an AMB system," *American Control Conference*, Baltimoer, MD, USA, 2010.

[3] A. Noshadi, J. Shi, W. S. Lee, P. Shi, and A. Kalam, "System identification and robust control of multi-input multi-output active magnetic bearing systems," *IEEE Transactions on Control Systems Technology*, vol. 24, no. 4, pp. 1227-1239, 2016.

[4] C. Gähler, M. Mohler, and R. Herzog, "Multivariable identification of active magnetic bearing systems," *JSME International Journal Series C Mechanical Systems, Machine Elements and Manufacturing*, vol. 40, no. 4, pp. 584-592, 1997.

[5] A. Wroblewski, J.T. Sawicki, and A. Pesch, "Rotor model updating and validation for an active magnetic bearing based high-speed machining spindle," ASME *Journal of Engineering for Gas Turbines and Power*, vol. 134, no. 12, 2012.

[6] A. Sahinkaya and J.T. Sawicki, "Application of genetic algorithm for synthesis of H_∞ controllers for active magnetic bearing Systems," *IFToMM 2018*, Rio de Janeiro, Brazil, 2018.

[7] J.T. Sawicki and E.H. Maslen, "AMB controller design for a machining spindle using μ-synthesis," The Tenth International Symposium on Magnetic Bearings (ISMB-10), Martigny, Switzerland, August 21-23, 2006.

[8] J.T. Sawicki and E.H. Maslen, "Toward automated AMB controller tuning: Progress in identification and synthesis," in *The 11th International Symposium on Magnetic Bearing (ISMB-11)*, Nara, Japan, 2008.

[9] L. Ljung, System Identification: Theory for the User, Second Edition, N.J: Prentice Hall, 1999.

[10] P. Van Overschee and B. De Moor, "N4SID: Subspace algorithms for the identification of combined deterministic-stochastic systems," *Automatica*, vol. 30, no. 1, pp. 75-93, 1994.

[11] M.H. Richardson and D.L. Formenti, "Global curve fitting of frequency response measurements using the rational fraction polynomial method," *3rd IMAC Conference*, Orlando, FL, 1985.

[12] J. Currie and D.I. Wilson, "OPTI: Lowering the barrier between open source optimizers and the industrial MATLAB user," *Foundations of Computer-Aided Process Operations*, 2012.

[13] S. Skogestad and I. Postlethwaite, Multivariable Feedback Control: Analysis and Design, 2nd ed., Chichester: John Wiley & Sons, 2007.